JPE 18-5-23

https://doi.org/10.6113/JPE.2018.18.5.1545
ISSN(Print): 1598-2092 / ISSN(Online): 2093-4718

Source Current Control Strategy of Active Power Filters for Unbalanced Load Compensation in Three-Phase Four-Wire Distribution Networks

Lei Wang*, Xiaoqing Han†, Runquan Meng*, Chunguang Ren*, Qi Wang*, and Baifu Zhang*

†,*Shanxi Key Lab of Power System Operation and Control, College of Electrical and Power Engineering, Taiyuan University of Technology, Taiyuan, China

Abstract

This paper proposes a modified control strategy to improve the performance of three-phase four-leg shunt active power filters (APFs) for the compensation of three phase unbalanced loads. Unbalanced current cannot be obtained accurately by a harmonic detector due to the lower frequency. The proposed control strategy eliminates conventional harmonic detectors by directly regulating the source current. Therefore, the computational complexity is greatly reduced and the performance of the APF is improved. A mathematic model has been developed based on the source currents. The corresponding controllers have been designed based on the sinusoidal internal model principle. The proposed control strategy can guarantee excellent compensation performance and stable operation after an extreme disturbance such as a short circuit fault. In addition, the proposed technique can selectively compensate specific harmonics. A 50kVA prototype APF is implemented in the laboratory to validate the feasibility and performance of the proposed control strategy.

Key words: Active Power Filter (APF), Source current control, Unbalanced load compensation

I. INTRODUCTION

Three-phase distribution networks usually operate under nonlinear and unbalanced conditions since there are a lot of unbalanced and nonlinear loads. System unbalanced operation can cause transmission loss and stability problems. Therefore, the maximum continuous unbalanced current is usually limited to within 10 percent in practical power systems [1]. A lot of equipment and techniques have been developed to alleviate unbalanced currents in distribution networks.

Many of the existing techniques are based on passive devices such as capacitors and inductors, which are suitable for fixed load conditions but are not flexible for time varying unbalanced loads [1]. In addition, passive equipment is large in size and slow in response. The aforementioned problems can be solved by using an active power filter (APF) [1]-[3]. The advantages of the APF include continuously balancing time varying loads, fast dynamic response to load variations and improved performance. The APF has been extensively studied [4], [5]. The harmonic components of load currents are continuously measured and compensated through the injection of the same amount of the opposite harmonic current by an APF at the Point of Common Coupling (PCC). Harmonic detection is a key factor for achieving better performance from APFs. Many different detection methods for APFs have been proposed.

Instantaneous Reactive Power Theory (IRPT) was used to extract harmonic components in [6]-[11]. The instantaneous harmonic power is extracted with a low-pass filter (LPF) [6]. In [7], the IRPT method was extended to three-phase four-wire power systems. However, the performance of an IRPT-based APF is limited since the distorted supply voltages influence the accuracy of the instantaneous powers and the reference currents. The synchronous reference frame (SRF) has also been proposed for extracting harmonic components [3] [12]-[16]. In [3], the load currents were transformed into *d-q* coordinates through a Park transformation, and a

Manuscript received Apr. 20, 2018; accepted Jun. 21, 2018
Recommended for publication by Associate Editor Kai Sun.
†Corresponding Author: hanxiaoqing@tyut.edu.cn
Tel: +86-0351-6010051, Taiyuan University of Technology
*College of Electrical and Power Eng., Taiyuan Univ. of Tech., China

decoupled control scheme was proposed. The authors of [14] proposed a method to achieve the flexibility of selective compensation based on the SRF, which can selectively compensate the harmonics, reactive current and negative sequence fundamental current of the load current. However, the performance of the two above methods for extracting harmonics depends on the performance of the LPF in the harmonic detector. There is a tradeoff between the accuracy and the dynamic response speed. It is more difficult to extract unbalanced components by a harmonic detector since unbalanced current has a lower frequency than harmonic.

Recently, neural networks, adaptive predictive control and various complex algorithms have been employed to improve the performance of harmonic detectors [17]-[21]. However, these intelligent algorithms increase the difficulty of design and require more computation resources from the controller.

A simple one cycle control (OCC) has been applied to APFs [22]-[25]. The OCC can be realized by a simple circuit. The most attractive advantage is that no harmonic detector is required. However, it has a constraint since the source currents after compensation are distorted, following the zero-sum components of the voltages [24], when the supply voltages are distorted.

Power-balance schemes have been proposed without harmonic detector [26]-[29]. However, there is no proper control scheme for three-phase four-wire systems with neutral compensation. Moreover, this control strategy suffers from a slow response to startups and sudden load changes. The capacitor voltage on the dc side of the APF may fluctuate acutely due to load changes.

This paper proposes an improved control strategy to balance the supply currents of three-phase four-wire distribution networks. This control strategy removes the harmonic detector by directly regulating the source currents. A mathematic model of the source currents-based control strategy is presented and the proposed strategy is theoretically derived in detail. The corresponding controllers have been designed based on the presented model. Compared with the conventional methods, the proposed control strategy has excellent performance in terms of compensating unbalanced currents and a fast dynamic response. It also has the capability of selective compensation.

II. Proposed Control Strategy

A. Modified Model of a Four-Leg APF

Fig. 1 shows a three-phase four-wire distribution network with unbalanced and nonlinear loads, which is connected in parallel with a four-leg shunt APF. The neutral leg of the APF is connected to the neutral wire at the PCC for suppressing zero-sequence current. In Fig. 1, R represents the total equivalent resistance on the ac side, L and C represent

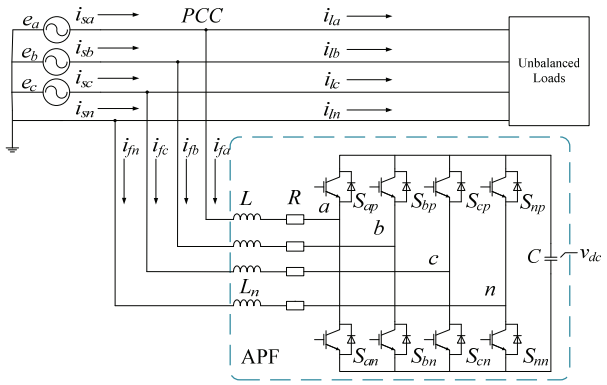

Fig. 1. Three-phase unbalanced load and a three-phase four-leg shunt APF.

inductance and capacitance, v_{dc} is the capacitor voltage on the dc side, (i_{sa}, i_{sb}, i_{sc}, i_{sn}), (i_{la}, i_{lb}, i_{lc}, i_{ln}) and (i_{fa}, i_{fb}, i_{fc}, i_{fn}) are three phase and neutral currents on the source, load and filter sides, and (S_{ap}, S_{bp}, S_{cp}, S_{np}) and (S_{an}, S_{bn}, S_{cn}, S_{nn}) are the upper switches and lower switches of the four legs, respectively.

When the d-axis is selected in phase with e_a, the differential equations of the APF are transformed in d-q-0 coordinates as [30]:

$$\begin{aligned} L\frac{di_{fd}}{dt} &= e_d + \omega L i_{fq} - R i_{fd} - v_{dc} d_d \\ L\frac{di_{fq}}{dt} &= e_q - \omega L i_{fd} - R i_{fq} - v_{dc} d_q \\ L\frac{di_{f0}}{dt} &= e_0 - R i_{f0} - v_{dc} d_0 + v_{dc} d_n + L_n \frac{di_{fn}}{dt} + R i_{fn} \\ C\frac{dv_{dc}}{dt} &= \left(\frac{3}{2} d_d i_{fd} + \frac{3}{2} d_q i_{fq} + 3 d_0 i_{f0}\right) + d_n i_{fn} \end{aligned} \tag{1}$$

where the subscripts d, q, 0 and n denote the d-axis, q-axis, 0-axis and neutral line, (d_d, d_q, d_0, d_n) and (i_{fd}, i_{fq}, i_{f0}) are the duty ratios for the switches and inductor currents in d-q-0 coordinates, and ω is the angular synchronous speed.

When the APF operates in the steady state, the filter currents have no dc components in d-q-0 coordinates and the dc operating point does not exist. Therefore, it is difficult to obtain a small signal model for the controller design. In order to avoid this problem, a modified model based on the source currents is developed. The fluctuating load currents are considered to be disturbances, and the source currents are treated as state variables. Both the loads and the APF are included in the system model.

The current equations at the PCC are:

$$i_{fd} = i_{sd} - i_{ld},\ i_{fq} = i_{sq} - i_{lq},\ i_{f0} = i_{s0} - i_{l0} \quad \text{and} \quad i_{fn} = i_{sn} - i_{ln} \tag{2}$$

where (i_{sd}, i_{sq}, i_{s0}, i_{sn}) and (i_{ld} i_{lq}, i_{l0}, i_{ln}) are the source and load currents in the d-q-0 coordinates, respectively. The source, load and filter currents in the 0-axis are:

$$i_{f0} = -\frac{1}{3} i_{fn},\ i_{s0} = -\frac{1}{3} i_{sn} \quad \text{and} \quad i_{l0} = -\frac{1}{3} i_{ln} \tag{3}$$

Substituting (2) and (3) into (1), the system differential equations become:

$$\frac{d}{dt}\begin{bmatrix} i_{sd} \\ i_{sq} \\ i_{sn} \\ v_{dc} \end{bmatrix} = \begin{bmatrix} -\frac{R}{L} & \omega & 0 & -\frac{d_d}{L} \\ -\omega & -\frac{R}{L} & 0 & -\frac{d_q}{L} \\ 0 & 0 & \frac{4/3\,R}{(L_n+1/3L)} & -\frac{d_n}{(L_n+1/3L)} \\ \frac{3d_d}{2C} & \frac{3d_q}{2C} & \frac{d_n}{C} & 0 \end{bmatrix} \begin{bmatrix} i_{sd} \\ i_{sq} \\ i_{sn} \\ v_{dc} \end{bmatrix} + \begin{bmatrix} \frac{e_d}{L} \\ \frac{e_q}{L} \\ -\frac{e_0}{(L_n+1/3L)} \\ 0 \end{bmatrix} + P,$$

$$P = \begin{bmatrix} \frac{di_{ld}}{dt} - \omega i_{lq} + \frac{Ri_{ld}}{L} \\ \frac{di_{lq}}{dt} + \omega i_{ld} + \frac{Ri_{lq}}{L} \\ \frac{v_{dc}d_0}{(L_n+1/3L)} + \frac{di_{ln}}{dt} + \frac{4/3\,Ri_{ln}}{(L_n+1/3L)} \\ -\frac{3}{2C}d_d i_{ld} - \frac{3}{2C}d_q i_{lq} - \frac{1}{C}d_n i_{ln} + \frac{3}{C}d_0\left(i_{s0} - i_{l0}\right) \end{bmatrix} \quad (4)$$

where P is a perturbation. (i_{sd}, i_{sq}, i_{sn}) are the state variables which can be controlled directly by the input variables (d_d, d_q, d_n). The modified model is suitable for a source currents-based control strategy without harmonic detection.

B. Source Currents-Based Direct Control Scheme

Model (4) is a coupled system with a perturbation. Define the equivalent control variables d_{d1}, d_{q1} and d_{n1} as follows:

$$\begin{aligned} d_d &= d_{d1} + \frac{\omega L i_{sq}}{v_{dc}} + \frac{e_d}{v_{dc}} + \frac{1}{v_{dc}}\left(\frac{Ldi_{ld}}{dt} - \omega L i_{lq} + Ri_{ld}\right) \\ d_q &= d_{q1} - \frac{\omega L i_{sd}}{v_{dc}} + \frac{e_q}{v_{dc}} + \frac{1}{v_{dc}}\left(\frac{Ldi_{lq}}{dt} + \omega L i_{ld} + Ri_{lq}\right) \\ d_n &= d_{n1} - \frac{e_0}{v_{dc}} + \frac{1}{v_{dc}}\left(\frac{(L_n+1/3L)di_{ln}}{dt} + \frac{4}{3}Ri_{ln}\right) \end{aligned} \quad (5)$$

Substituting (5) into (4), the coupled system is transformed into three independent decoupled systems, and the source currents can be directly controlled by (d_{d1}, d_{q1}, d_{n1}). A model of the current control loop can be obtained by a transformation. Considering the digital cycle delay and the PWM modulation, block diagrams of the current control loop are shown in Fig. 2, where i_{sdref}, i_{sqref} and i_{snref} represent the source reference currents in three axes, T_s is the switching period, and $N(s)_d$, $N(s)_q$ and $N(s)_n$ are disturbances in the s domain, which are composed of unbalanced and nonlinear load currents as follows:

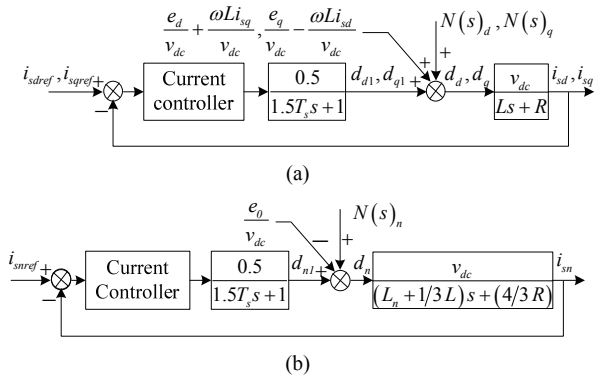

Fig. 2. Block diagram of the current control loop: (a) In the *d* and *q* axis, (b) In the *0* axis.

$$\begin{aligned} N(s)_d &= \frac{1}{v_{dc}}\left(Li_{ld}s - \omega Li_{lq} + Ri_{ld}\right) \\ N(s)_q &= \frac{1}{v_{dc}}\left(Li_{lq}s + \omega Li_{ld} + Ri_{lq}\right) \\ N(s)_n &= \frac{1}{v_{dc}}\left(\left(L_n+1/3L\right)i_{ln}s + \frac{4}{3}Ri_{ln}\right) \end{aligned} \quad (6)$$

According to the current control loop in Fig. 2, $N(s)_d$, $N(s)_q$ and $N(s)_n$ may lead to undesirable errors of i_{sd}, i_{sq} and i_{sn}. In essence, $N(s)_d$, $N(s)_q$ and $N(s)_n$ are sinusoidal waves at multiple frequencies. Based on the sinusoidal internal model principle [31], the controller can erase disturbances if it includes transfer functions of the disturbances. Therefore, the current controller is designed to be a sinusoidal transfer function with multiple frequencies as:

$$G_C(s) = \frac{k_{rn}s}{s^2 + (n\omega)^2} \quad (7)$$

where k_{rn} is the controller gain, and $n\omega$ are the angular speeds which correspond with the frequencies of disturbances.

Assuming that the loads are composed of unbalanced resistors and three-phase diode rectifiers, the load currents include the ($6n\pm1$) harmonics and fundamental current, and the frequencies of the load currents change in the synchronous coordinate. In the *d* and *q* axis, the positive-sequence n^{th} harmonics are transformed into $(n\text{-}1)^{th}$, and the negative-sequence n^{th} harmonics are transformed into $(n+1)^{th}$. Meanwhile, in the *0* axis the frequencies remain unchanged. In addition, in many instances the $3n^{th}$ harmonics exist in the *0* axis. The frequencies distribution of the load currents in the synchronous coordinate are shown in Fig. 3. In order to eliminate disturbances with different frequencies, the corresponding current controller (7) for each of the disturbances is designed. A control scheme with current controller (7) having enough gain at the $n\omega$ frequencies can ensure that the steady-state errors become zero. Hence, the designed current controllers can remove the effects of disturbances at specified frequencies.

In practice, three-phase distribution systems usually have slight frequency deviations [32]. Therefore, the current

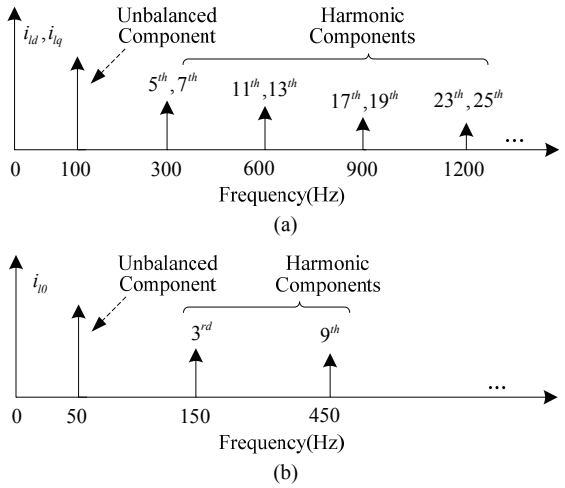

Fig. 3. Frequencies distribution of the loads currents in Park's coordinates: (a) In the *d* and *q* axis, (b) In the *0* axis.

controller (7) is modified to avoid frequency deviations by increasing the bandwidth of a specified frequency. With the proportional and integral control, the current controller becomes:

$$G_C(s) = k_{pc} + \frac{k_{ic}}{s} + \sum \frac{k_{rn} s}{s^2 + \omega_c s + (n\omega)^2} \tag{8}$$

where k_{pc} and k_{ic} are the coefficients of the proportional and integral control, and ω_c is the bandwidth of the specified frequency. In the proposed current control scheme, the source currents are regulated directly without harmonic detection. In addition, this control scheme can selectively compensate a specific harmonic if a current controller corresponding with the frequencies of the specific harmonic is designed.

C. Voltage Control and Dynamic Response

For the voltage control loop, the equivalent transformation is defined as:

$$i_{sd} = i_{sd1} + i_{ld} - \frac{d_q i_{sq}}{d_d} + \frac{d_q i_{lq}}{d_d} + \frac{2}{3}\left(\frac{d_n i_{sn}}{d_d} - \frac{d_n i_{ln}}{d_d}\right) \tag{9}$$

where i_{sd1} is the equivalent control variable. Substituting (9) into (4), the voltage control loop is derived as shown in Fig. 4, where v_{dcref} represents the dc reference voltage, $C_c(s)$ represents the closed-loop transfer function of the current control loop, and $N(s)_v$ is as follows:

$$N(s)_v = \frac{d_q i_{lq}}{d_d} - \frac{d_q i_{sq}}{d_d} + \frac{2}{3}\left(\frac{d_n i_{sn}}{d_d} - \frac{d_n i_{ln}}{d_d}\right) \tag{10}$$

Fig. 4 shows that the voltage controller and current control loop form a dual closed-loop control structure. $N(s)_v$ and i_{ld} lead to an undesirable error of the dc voltage. There are two types of disturbances that affect the dc voltage. The first is steady state disturbances and the second is transient disturbances such as sudden changes of the load.

Steady state disturbances result in a regular ripple of the dc voltage. In terms of the power flow theory for APF operation,

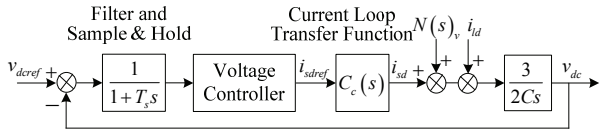

Fig. 4. The block diagram of the voltage control loop.

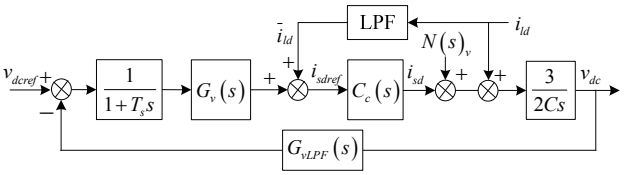

Fig. 5. The block diagram of the proposed voltage control scheme.

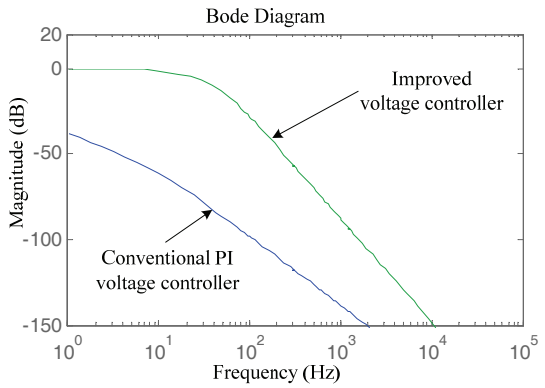

Fig. 6. Bode diagram of $H_i(s)$ with two voltage controllers.

the harmonics of the load currents cannot be completely compensated with non-ripple of the dc voltage. Therefore, the ripple is inevitable. The voltage regulator needs a simple PI controller (11) to keep the system operating stably.

$$G_v(s) = k_{pdc} + \frac{k_{idc}}{s} \tag{11}$$

where k_{pdc} and k_{idc} are the coefficients of the proportional and integral, respectively. In order to relieve the effects of the ripple on the current loop in the steady state, a one-order LPF is employed to remove all of the ripples in the feedback measurement of the dc voltage, as follows:

$$G_{vLPF}(s) = \frac{1}{1/\omega_{cL}\, s + 1} \tag{12}$$

where ω_{cL} is the cutting frequency of the LPF.

Transient disturbances can lead to acute fluctuations of the dc voltage of the APF. If the system operates in the steady state, only the ac source supplies active power, and the APF provides the reactive and harmonic power. In addition, if the load active power changes, the source reference current i_{sdref} in accordance with the active power supplied by the ac source should follow the variations of the load power. However, the PI voltage controller (11) and LPF (12) are tuned for a slow dynamic response in order to avoid interference from the dc voltage. Therefore, i_{sdref}, as the output of the voltage controller, cannot immediately follow abrupt variations of the load active power. Then the incremental load active power cannot be supplied by

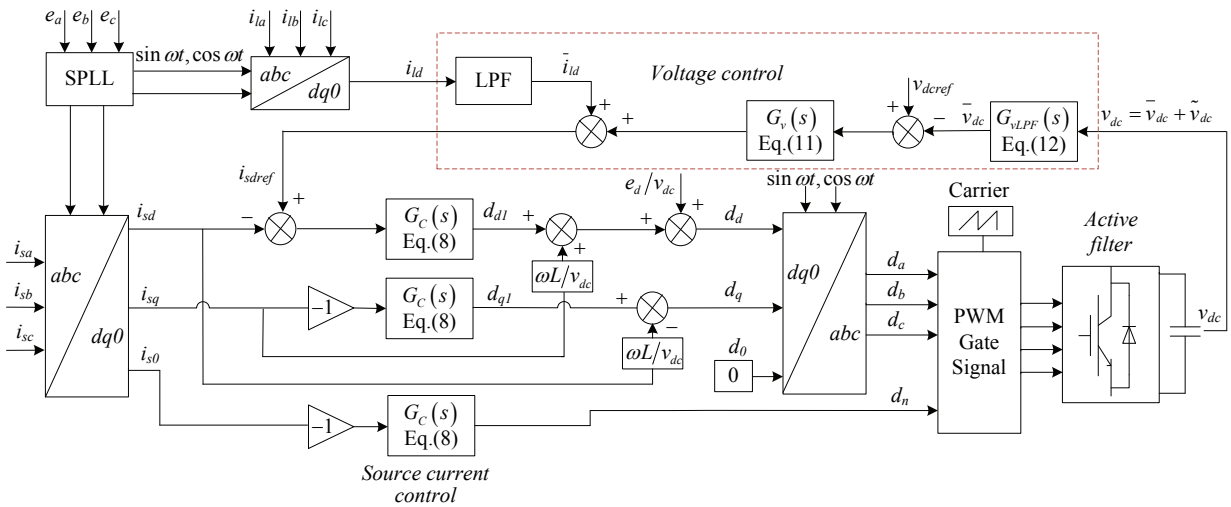

Fig. 7. Proposed control scheme for a three-phase four-leg shunt APF.

the ac source. Instead, it is supplied by the dc-link capacitor of the APF. Therefore, dc voltage fluctuates acutely, and may heavily impact the normal operation of the APF, especially under the unbalanced load conditions.

The proposed voltage control scheme can eliminate these defects. A second-order LPF is applied to obtain the dc component of the load current. The voltage control scheme is depicted as shown in Fig. 5.

This figure shows that the active component of the load current is feedforward. The transfer function between i_{ld} and i_{sdref} is derived as:

$$H_i(s)=\frac{\omega_n^2}{s^2+\sqrt{2}/2\,\omega_n s+\omega_n^2} - \frac{\frac{3}{2Cs}\cdot G_{vLPF}(s)\cdot\frac{1}{1+T_s s}\cdot G_v(s)}{1+\frac{3}{2Cs}\cdot G_{vLPF}(s)\cdot\frac{1}{1+T_s s}\cdot G_v(s)\cdot C_c(s)} \quad (13)$$

where ω_n is the cutting angular frequency of the second-order LPF. Fig. 6 shows a Bode diagram of $H_i(s)$. When compared with the conventional PI voltage controller, the voltage control scheme with feedforward compensation has a significantly faster dynamic response. Fig. 7 shows a block diagram of the proposed control strategy in detail.

III. Experiment Verification

An experiment platform has been set up, as shown in Fig. 8, to verify the performance of the proposed control scheme. This control scheme was implemented on a digital signal processor DSP (TMS320F28377D), with a 200MHz clock frequency. A software PLL is employed for improving flexibility. A chip (AD7606) is used in the control board due to the high demand for simultaneous signals sampling. The voltage signals are provided by LV 25-P LEM voltage sensors and the current signals are provided by LT 108-S7/sp1 Hall Effect current sensors. A Concept 2SC0108T is applied to drive the IGBTs. The switch frequency is 12.8 kHz. The unbalanced loads are composed of resistors, and the nonlinear loads are composed of a three-phase diode rectifier with resistors in the dc side. The ac power supply is an autotransformer. The experimental parameters are shown in Table I. The controller gains are tuned, and are modified by HMI.

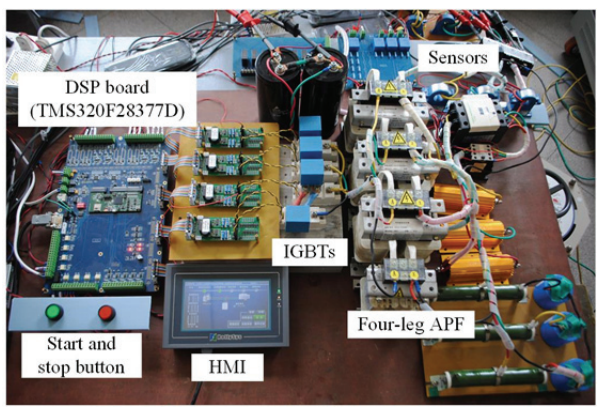

Fig. 8. Hardware platform of the proposed system.

TABLE I
Experiment Parameters

Parameters	Hardware platform	Prototype
Supply voltage	120V/50Hz	220V/50Hz
Inductor	L=3mH, L_n=0.3mH	L=L_n=1mH,
DC side capacitor	5000μF	6600μF
Switch frequency	12.8kHz	12.8kHz
Dc reference voltage	415V	800V
Voltage loop PI	K_p=0.1, K_i=0.2	K_p=0.1, K_i=0.2
Current loop PI	K_p=0.15, K_i=0.2	K_p=0.1, K_i=0.15
Current loop resonant gains in d and q axis	K_{r2}=5, K_{r6}=5, K_{r12}=5, K_{r18}=3	K_{r2}=5, K_{r6}=5, K_{r12}=5, K_{r18}=3
Current loop resonant gains in 0 axis	K_{r1}=5, K_{r3}=10, K_{r9}=3	K_{r1}=5, K_{r3}=10, K_{r9}=3

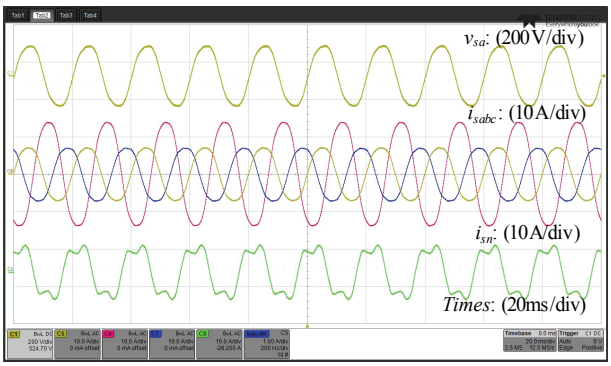

Fig. 9. Experimental waveforms of the unbalanced source currents.

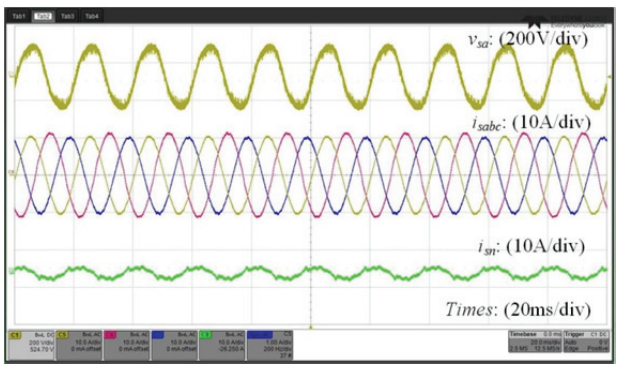

(a)

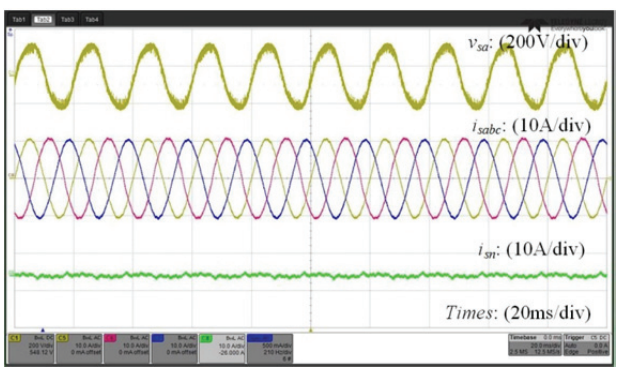

(b)

Fig. 10. Experimental waveforms with two methods after compensation: (a) Harmonic detection method, (b) Proposed control strategy.

The proposed control strategy is compared with the traditional harmonic detection method. Fig. 9 shows i_{sa}, i_{sb}, i_{sc} and i_{sn} before compensation and the unbalanced rate is about 50%. Fig. 10(a) shows the performance of the harmonic detection method based on the SRF. The LPF, which is a key part in the harmonic detector, is a second-order filter with a 25Hz cutting frequency. i_{sa}, i_{sb} and i_{sc} are still unbalanced and i_{sn} is small after compensation. The currents unbalance rate is about 7%. Fig. 10(b) shows the performance of the proposed control scheme under the same conditions. Obviously i_{sa}, i_{sb} and i_{sc} are almost balanced and i_{sn} is reduced to almost zero. The unbalanced rate is decreased to about 1.2%. These experiment results show that the proposed control scheme is superior for compensating unbalanced currents.

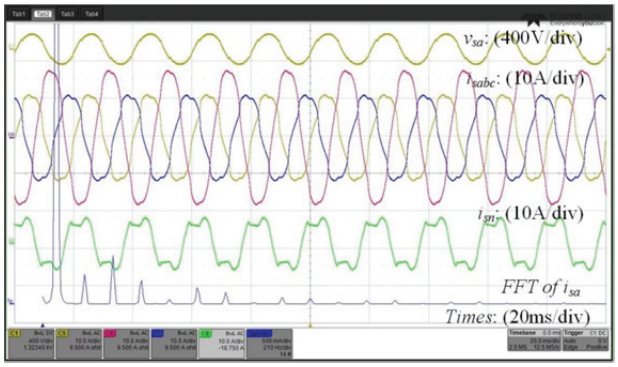

(a)

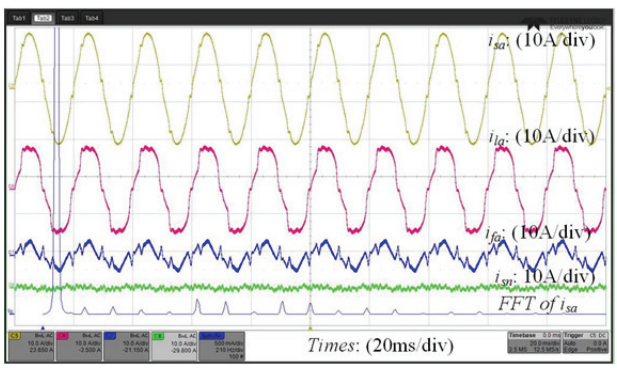

(b)

Fig. 11. Experimental waveforms of the proposed control strategy under unbalanced and nonlinear loads: (a) Before compensation, (b) After compensation.

Fig. 11 shows the performance of the proposed control scheme under the unbalanced and nonlinear load condition. Fig. 11(a) shows voltage and current waveforms before compensation. It can be seen that i_{sa}, i_{sb} and i_{sc} contain an amount of the 3rd, 5th, 7th harmonic and unbalanced components. The Total Harmonic Distortion (THD) is about 13%. After compensation, as shown in Fig. 11(b), i_{sa} is sinusoidal and i_{sn} is almost zero. The THD decreases to 3.2%.

Fig. 12 shows the performance of selectively compensating a specific harmonic. Fig. 12(a) shows the performance where only a harmonic is compensated and unbalanced components retain after compensation. i_{sa} is regulated to be sine shaped and i_{sn} retains the fundamental component due to three-phase unbalanced load currents. Fig. 12(b) shows the performance of compensation excluding the 3rd harmonic. It can be seen from the FFT spectrum at the bottom of Fig. 12(b) that i_{sa} includes an amount of the 3rd harmonic. In addition, i_{sn} is almost composed of the 3rd harmonic. These results verify that the proposed control scheme has excellent performance in terms of selective compensation.

Experiments on startup and during a sudden change of loads are carried out. Fig. 13 shows the transient process when an APF is applied. It can be seen that i_{fa} quickly responds to compensate the harmonic currents and that i_{sa} is well regulated within one period of the fundamental current. Importantly,

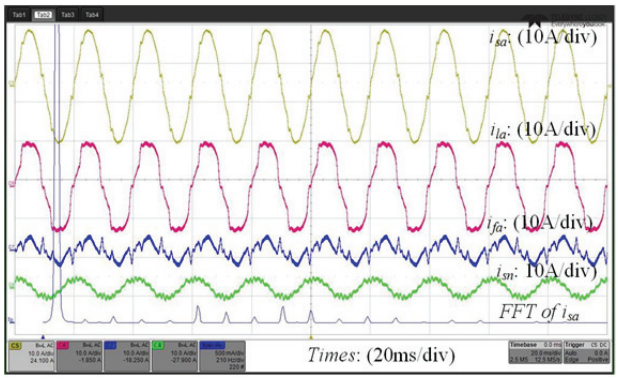

(a)

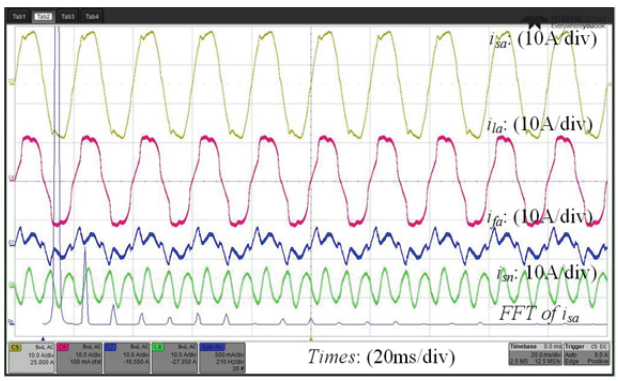

(b)

Fig. 12. Experimental waveforms of compensating a specific harmonic: (a) Retaining the unbalanced component, (b) Retaining the 3rd harmonic.

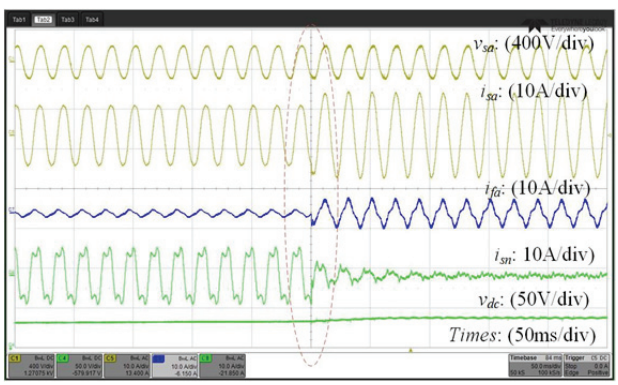

Fig. 13. Transient experimental waveforms when an APF applied.

during the process of startup, i_{sa} is kept stable without a startup shock and v_{dc} is kept constant without a leap. Fig. 14 shows dynamic response when the load currents change suddenly. An extreme case is considered where i_{la} changes acutely from 9A to 0A and from 0A to 9A. It can be seen that the system responds quickly to load variations during this process. i_{sa} is regulated without shock. v_{dc} fluctuates less than 7V and is rapidly restored back to normal.

It can be seen from Figs. 9-14 that the proposed control scheme has excellent performance in three-phase four-wire systems, especially when it comes to compensating unbalanced loads.

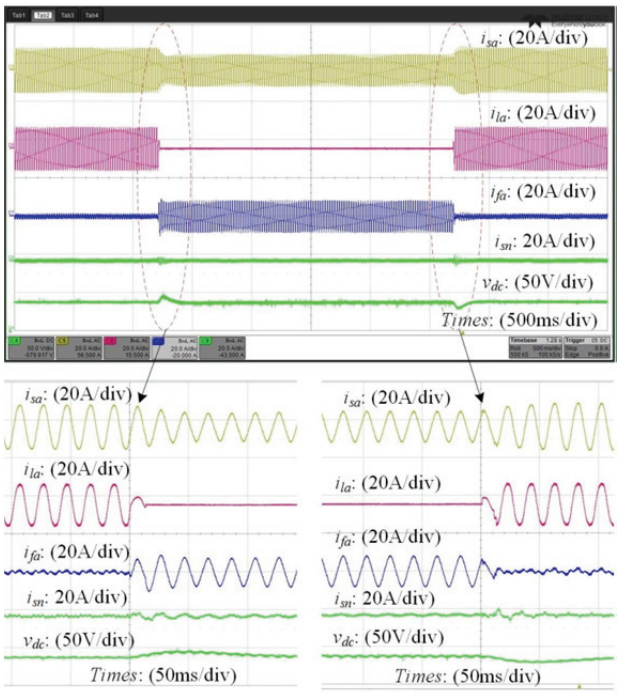

Fig. 14. Transient experimental waveforms when the load changes.

(a)

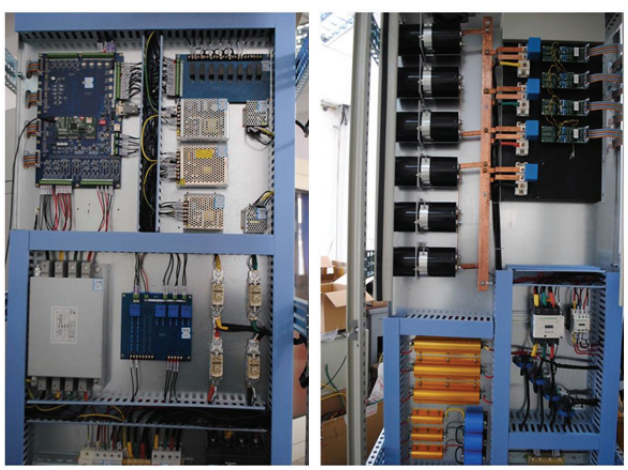

(b) (c)

Fig. 15. Prototype of the proposed system: (a) Under test, (b) DSP-based control system, (c) Main converter.

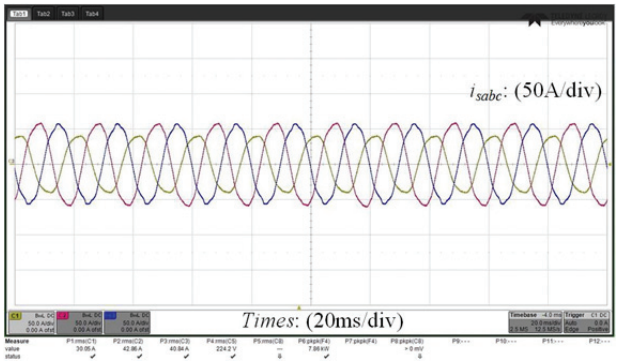

(a)

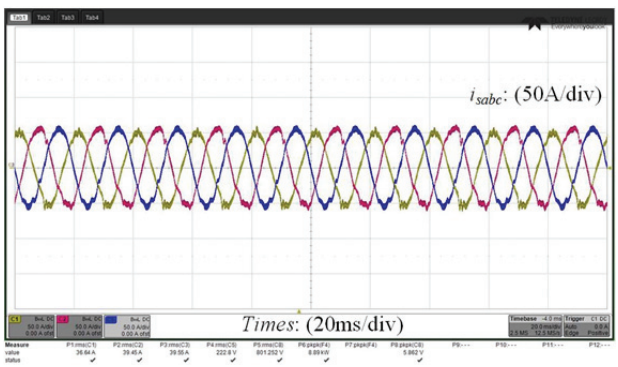

(b)

Fig. 16. Test results: (a) Before the system runs, (b) After the system runs.

IV. Prototype Implementation

A 50kVA prototype with the proposed control strategy has been implemented in a practical distribution network for testing and commissioning. Fig. 15 shows the prototype and its internal structure, which is supplemented with indispensable startup circuits and protective circuits. The main converter uses Infineon FF150R12RT4 IGBTs for 1200V/150A. The supply voltage is 220V/50Hz and the dc reference voltage is set to 800V. The detailed parameters are shown in Table I. Fig. 16 shows test results of compensating unbalanced loads. i_{sa}, i_{sb} and i_{sc} are improved from (30A, 43A, 41A) to (37A, 39A, 39A).

V. Conclusions

Unlike harmonics, unbalanced currents have a lower frequency. Conventional harmonic detection methods cannot accurately obtain the compensation reference current. This paper proposed a modified control strategy to improve the performance of APFs for compensating three phase unbalanced load currents. This control strategy removes the harmonic detector by directly regulating the source current. A mathematic model for the source currents-based direct control strategy is developed and the corresponding controllers have been designed based on this model. Experimental results show that the proposed control strategy significantly improves the compensation precision of the APF when compared with the conventional method, especially for compensating unbalanced load currents. It also has the superiority ability to selectively compensating specific harmonic. Meanwhile, the elimination of the harmonic detector reduces the computational complexity. A 50kVA prototype has been implemented and connected to the grid for testing and commissioning. The test results of the prototype confirm that the proposed control strategy can be applied successfully to APFs and that is has satisfactory performance.

Acknowledgment

Financial Supports from National Key R&D Program of China (2018YFB0904700), National Natural Science Foundation of China (51777132), National Natural Science Foundation of China (U1610121), Shanxi Province Applied Basic Research project (201701D121134), and State Grid Shanxi Electric Power Company Science and Technology Project Research (52053017000G) are gratefully acknowledged.

References

[1] V. B. Bhavaraju and Prasad N. Enjeti, "Analysis and design of an active power filter for balancing unbalanced loads," *IEEE Trans. Power Electron.*, Vol. 8, No. 4, pp. 640-647, Oct. 1993.

[2] H. Akagi, "New trends in active filters for power conditioning," *IEEE Trans. Ind. Appl.*, Vol. 32, No. 2, pp. 1312-1332, Nov./Dec. 1996.

[3] P. Verdelho and G. D. Marques, "An active power filter and unbalanced current compensator," *IEEE Trans. Ind. Electron.*, Vol. 44, No. 3, pp. 321-328, Jun. 1997.

[4] B. Singh, K. Al-Haddad, and A. Chandra, "A review of active filters for power quality improvement," *IEEE Trans. Ind. Electron.*, Vol. 46, No. 5, pp. 960-971, Oct. 1999.

[5] L. Asiminoaei, F. Blaabjerg, and S. Hansen, "Detection is key—Harmonic detection methods for active power filter applications," *IEEE Ind. Appl. Mag.*, Vol. 13, No. 4, pp. 22-33, Jul./Aug. 2007.

[6] M. Aredes, J. Häfner, and K. Heumann, "Three-phase four-wire shunt active filter control strategies," *IEEE Trans. Power Electron.*, Vol. 12, No. 2, pp. 311-318, Mar. 1997.

[7] F. Z. Peng, G. W. Ott, and D. J. Adams, "Harmonic and reactive power compensation based on the generalized instantaneous reactive power theory for three-phase four-wire systems," *IEEE Trans. Power Electron.*, Vol. 13, No. 5, pp. 1174-1181, Nov. 1998.

[8] G. W. Chang and T.-C. Shee, "A novel reference compensation current strategy for shunt active power filter control," *IEEE Trans. Power Del.*, Vol. 19, No. 4, pp. 1751-1758, Oct. 2004.

[9] H. Li, F. Zhuo, Z. Wang, W. Lei, and L. Wu, "A novel time-domain current-detection algorithm for shunt active power filters," *IEEE Trans. Power Syst.*, Vol. 20, No. 2, pp. 644-651, May 2005.

[10] R. S. Herrera and P. Salmeron, "Instantaneous reactive power theory: A reference in the nonlinear loads compensation," *IEEE Trans. Ind. Electron*., Vol. 56, No. 6, pp. 2015-2022, Jun. 2009.
[11] R. S. Herrera, P. Salmeron, and K. Hyosung, "Instantaneous reactive power theory applied to active power filter compensation: Different approaches, assessment, and experimental results," *IEEE Trans. Ind. Electron*., Vol. 55, No. 1, pp. 184-196, Jan. 2008.
[12] M. J. Newman, D. N. Zmood, and D. G. Holmes, "Stationary frame harmonic reference generation for active filter systems," *IEEE Trans. Ind. Appl.*, Vol. 38, No. 6, pp. 1591-1599, Nov./Dec. 2002.
[13] M. Kesler and E. Ozdemir, "Synchronous-reference-frame-based control method for UPQC under unbalanced and distorted load conditions," *IEEE Trans. Ind. Electron*., Vol. 58, No. 9, pp. 3967-3975, Sep. 2011.
[14] B. Singh and V. Verma, "Selective compensation of power-quality problems through active power filter by current decomposition," *IEEE Trans. Power Del.*, Vol. 23, No. 2, pp. 792-799, Apr. 2008.
[15] S. Rahmani, N. Mendalek, and K. Al-Haddad, "Experimental design of a nonlinear control technique for three-phase shunt active power filter," *IEEE Trans. Ind. Electron.*, Vol. 57, No. 10, pp. 3364-3375, Oct. 2010.
[16] H. Haibing and X. Yan, "Design considerations and fully digital implementation of 400-Hz active power filter for aircraft applications," *IEEE Trans. Ind. Electron*., Vol. 61, No. 8, pp. 3823-3834, Aug. 2014.
[17] A. Bhattacharya and C. Chakraborty, "A shunt active power filter with enhanced performance using ANN-based predictive and adaptive controllers," *IEEE Trans. Ind. Electron*., Vol. 58, No. 2, pp. 421-428, Feb. 2011.
[18] M. Qasim, P. Kanjiya, and V. Khadkikar, "Artificial-neural-network based phase-locking scheme for active power filters," *IEEE Trans. Ind. Electron.*, Vol. 61, No. 8, pp. 3857-3866, Aug. 2014.
[19] P. Kanjiya, V. Khadkikar, and H. H. Zeineldin, "Optimal control of shunt active power filter to meet IEEE Std. 519 current harmonic constraints under nonideal supply condition," *IEEE Trans. Ind. Electron.*, Vol. 62, No. 2, pp. 724-734, Feb. 2015.
[20] P. Kanjiya, V. Khadkikar, and H. H. Zeineldin, "A noniterative optimized algorithm for shunt active power filter under distorted and unbalanced supply voltages," *IEEE Trans. Ind. Electron*., Vol. 60, No. 12, pp. 5376-5390, Dec. 2013.
[21] Z. Zou, K. Zhou, Z. Wang, and M. Cheng, "Frequency adaptive fractional order repetitive control of shunt active power filters," *IEEE Trans. Ind. Electron*., Vol. 62, No. 3, pp. 1659-1668, Mar. 2015.
[22] K. M. Smedley, L. Zhou, and C. Qiao, "Unified constant-frequency integration control of active power filters-steady-state and dynamics," *IEEE Trans. Power Electron.*, Vol. 16, No. 3, pp. 428-436, May 2001.
[23] L. Wang, X. Han, C. Ren, Y. Yang, and P. Wang, "A modified one-cycle-control-based active power filter for harmonic compensation," *IEEE Trans. Ind. Electron*., Vol. 65, No. 1, pp. 738-748, Jan. 2018.
[24] J. Taotao and K. M. Smedley, "Operation of one-cycle controlled threephase active power filter with unbalanced source and load," *IEEE Trans. Power Electron*., Vol. 21, No. 5, pp. 1403-1412, Sep. 2006.
[25] L. Wang, C. Ren, Y. Yang, X. Han, and P. Wang, "An improved one cycle control for active power filters under non-ideal voltage conditions," *J. Power Electron.*, Vol. 16, No. 6, pp. 2350-2358, Nov. 2016.
[26] H. Yi, F. Zhuo, Y. Zhang, Y. Li, W. Chen, and J. Liu, "A source-current-detected shunt active power filter control scheme based on vector resonant controller," *IEEE Trans. Ind. Appl.*, Vol. 50, No. 3, pp. 1953-1965, May/Jun. 2014.
[27] R. L. de Araujo Ribeiro, T. de Oliveira Alves Rocha, R. M. de Sousa, E. C. dos Santos, Jr., and A. M. Nogueira Lima, "A robust DC-link voltage control strategy to enhance the performance of shunt active power filters without harmonic detection schemes," *IEEE Trans. Ind. Electron.*, Vol. 62, No. 2, pp. 803-813, Feb. 2015.
[28] Q.-N. Trinh and H.-H. Lee, "An advanced current control strategy for three-phase shunt active power filters," *IEEE Trans. Ind. Electron*., Vol. 60, No. 12, pp. 5400-5410, Dec. 2013.
[29] M. Angulo, J. Lago, D. Ruiz-Caballero, S. Mussa, and M. Heldwein, "Active power filter control strategy with implicit closed loop current control and resonant controller," *IEEE Trans. Ind. Electron*., Vol. 6, No. 7, pp. 2721-2730, Jul. 2013.
[30] H. Y. Kanaan, K. Al-Haddad, A. A. Assi, J. B. Sleiman, M. Aoun, and C. Asmar, "Averaged modeling and control of a three-phase series active power filter for voltage harmonic compensation," in *Proc. IEEE 29th Annu. Conf. Industrial Electronics Soc*., Vol. 1, pp. 255-260, 2003.
[31] S. Fukuda and T. Yoda, "A novel current-tracking method for active filters based on a sinusoidal internal model," *IEEE Trans. Ind. Appl*., Vol. 37, No. 3, pp. 888-895, May 2001.
[32] S. Fukuda and R. Imamura, "Application of a sinusoidal internal model to current control of three-phase utility-interface converters," *IEEE Trans. Ind. Electron*., Vol. 52, No. 2, pp. 420-426, Apr. 2005.

Lei Wang was born in China, in 1985. He received his M.S. and Ph.D. degrees from the Taiyuan University of Technology, Taiyuan, China, in 2010 and 2017, respectively. He is presently working as an Assistant Professor in the College of Electrical and Power Engineering, Taiyuan University of Technology. His current research interests include power electronic converters, active and hybrid filters, the application of power electronics in renewable energy systems, and power quality compensation systems.

Xiaoqing Han received her B.S., M.S. and Ph.D. degrees from the College of Electrical and Power Engineering, Taiyuan University of Technology, Taiyuan, China. She is presently working as a Professor at the Taiyuan University of Technology. Her current research interests include power system simulation, stability analysis, and the integration of renewable energy sources. Professor Han was a recipient of a Science and Technology Award of Shanxi Province, in 2001 and 2005.

Runquan Meng received his B.S. degree from Department of Computer Science and Information Engineering, Hefei University of Technology, Hefei, China, in 1991; and his M.S. and Ph.D. degrees from the College of Electrical and Power Engineering, Taiyuan University of Technology, Taiyuan, China, in 1999 and 2010, respectively. He is presently working as an Associate Professor in the College of Electrical and Power Engineering, Taiyuan University of Technology. His current research interests include distributed generation, power quality and power converters.

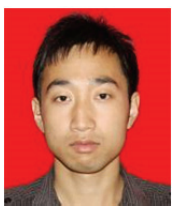

Chunguang Ren was born in China, in 1989. He received his M.S. and Ph.D. degrees from the College of Electrical and Power Engineering, Taiyuan University of Technology, Taiyuan, China, in 2012 and 2017, respectively. He is presently working as an Assistant Professor at the Taiyuan University of Technology. His current research interests include power electronic interfaces for the renewable sources in microgrids and the stability of power converters.

Qi Wang was born in China, in 1991. He received his M.S. degree from the Taiyuan University of Technology, Taiyuan, China, in 2015, where he is presently working towards his Ph.D. degree in the College of Electrical and Power Engineering. His current research interests include the robustness and stability of power electronic converters under weak grids and the resonance characteristics of power electronic converters in distribution systems.

Baifu Zhang was born in China, in 1992. He received his B.S. degree from the Taiyuan University of Technology, Taiyuan, China, in 2015, where he is presently working towards his Ph.D. degree in the College of Electrical and Power Engineering. His current research interests include power electronics for microgrids and distributed power generation.